Hindawi
Science and Technology of Nuclear Installations
Volume 2021, Article ID 8860762, 15 pages
https://doi.org/10.1155/2021/8860762

Research Article

A Novel and High-Precision Method for Calculating the γ-Ray Build-Up Factor for Multilayer Shields

Chao Li,[1] **Yingming Song**,[1,2] **Zehuan Zhang**,[1] **Jie Mao**,[1] **Weiwei Yuan**,[3] **and Bo Wang**[1]

[1]*School of Nuclear Science and Technology, University of South China, Hengyang, Hunan 421001, China*
[2]*National Exemplary Base for International Science and Technology Collaboration of Nuclear Energy and Nuclear Safety, University of South China, Hengyang, Hunan 421001, China*
[3]*Radon Provincial Key Laboratory, University of South China, Hengyang, Hunan 421001, China*

Correspondence should be addressed to Yingming Song; songyingming@tsinghua.org.cn

Received 15 September 2020; Accepted 13 January 2021; Published 27 January 2021

Academic Editor: Alexander Pavliuk

In the field of radiation protection, the point-kernel code method is a practical tool widely used in the calculation of 3-D radiation field, and the accuracy of the point-kernel integration method strongly depends on the accuracy of the build-up factor. It is well known that calculation of the build-up factor for single-layer shields is composed of single material, but it is very complicated to calculate the build-up factor for multilayer shields (MLBUF). Recently, a novel and high-precision method based on the deep neural network (DNN) for calculating MLBUF has been proposed. In this paper, the novel method is described completely by slab models. Through the study of photon transport in multilayer shields, the parameters that mainly affect the calculation of build-up factor are analyzed. These parameters are trained by DNN as the input vectors, and the build-up factor for multilayer shields is predicted based on the trained DNN. The results predicted by DNN confirm that the method can calculate the build-up factor for multilayer shields quickly and accurately. The method has been preliminarily applicated into a 3-D radiation field calculation software, and it has proved that the method for calculating MLBUF has a broad application prospects in 3-D radiation field calculation.

1. Introduction

To protect radiation protection personnel from the radiation harm, it is often necessary to know the radiation situation of the working environment in advance and calculate the distribution of 3-D radiation field quickly and accurately. At present, the main methods for calculating the 3-D radiation field are determination method, Monte Carlo method, and point-kernel method. Due to the fast calculation speed and being suitable to solve deep penetration problem, the point-kernel method [1, 2] shown in formula (1) is usually used in the calculation of 3-D radiation field, such as QAD [2], MICROSHEILD [3], MERCURE [4], and Monte Carlo coupling point-kernel method [5]. Although the point-kernel method can apply in 3-D radiation calculation at some extent, the radiation filed calculation results are highly relied on the estimated build-up factor [6, 7], and the error of calculation results brought by estimated build-up factor is relatively large, and calculation accuracy cannot satisfy the higher and higher accuracy requirement of practical engineering. This work is aimed to improve calculation accuracy of the build-up factor and ensure the accuracy of 3-D radiation field calculation in practical engineering application.

$$H(r) = F \iint_{EV} \frac{A(r', E)}{4\pi(r - r')^2} B(d, E) e^{-\mu(E)d} \mathrm{d}V \mathrm{d}E, \quad (1)$$

where $H(r)$ is the dose rate at the reference point r, $F$is the conversion factor of photon flux rate to dose rate, $A(r', E)$ is the source activity of specified energy located at r', d is the piercing path length along $r - r'$, $B(d, E)$ is the build-up factor, and $\mu(E)$ is the linear absorption coefficient.

A lot of efforts have been done to improve the accuracy calculation of build-up factors. The methods of calculating

build-up factor for single-layer shields have been very mature, and the empirical formulas, such as Taylor formula [8] shown in formula (2), interpolation method based on ANSI/ANS-6.4.3 [9] database, and G-P fitting formula [10] shown in (3) and (4) are usually used to calculate the build-up factor for single-layer shields.

$$B(E,\mu d) = \beta(E)e^{\left(-\alpha_1(E)\mu d\right)} + (1-\beta(E))e^{\left(-\alpha_2(E)\mu d\right)}, \quad (2)$$

where E is the energy of gamma-ray, μ is the mass attenuation coefficient of shielding, and α_1, α_2, and $\beta$are the functions of energy, and they are related to materials.

$$B(E,x) = \begin{cases} 1+(b-1)x & \text{for } K=1, \\ \dfrac{1+(b-1)\left(K^x-1\right)}{(K-1)} & \text{for } K\neq 1, \end{cases} \quad (3)$$

$$K(x) = cx^a + d\frac{\tan h\left(x/x_k - 2\right) - \tan h(-2)}{1-\tan h(-2)} \quad \text{for } X \leq 40, \quad (4)$$

where E is the energy of photon, $x$is the mean free path of photon, B is build-up factor, and b, c, a, and $x_k$are the parameters of the G-P fitting formula.

While for multilayer shields, whose each layer is composed of different materials or combinations of different materials, the transport process of photons in the multilayer shields is relatively complicated, and it is difficult to calculate the build-up factor with simple empirical formulas. In early stage, due to the limitation of computer technology, the calculation of build-up factor for muiltlayer shields mainly focused on empirical formulas fitting, mainly including Kalos formula [11], Bowman and Trubey formula [12], Broder formula [13], Burke and Beck formula [14], and Lin and Jiang formula [15]. In addition, a useful and free online platform called Py-MLBUF [16] for calculating the build-up factor is available. It includes the most of empirical formulas, and it can select different empirical formulas to calculate fastly the build-up factor on the basis of requirement. With the rapid development of computer science and technology, the researchers proposed the iterative algorithm [17] and support vector regression (SVR) [18] method to achieve the accurate calculation of build-up factors for muiltlayer shields. Although the methods mentioned above achieved some good results, it cannot satisfy today's requirement in practical engineering application. For empirical and semiempirical, the main problems are the necessity of defining the fitting function specially and a large number of correction factors are often added in the final empirical formula, which are usually not fully explained and inadequately defined [18]. As for the SVR and iterative method, their calculation accuracy was seem not far from acceptable, but they cannot satisfy the higher and higher accuracy requirement of practical engineering application. Therefore, how to calculate more accurately the build-up factor for multilayer shields has been an urgent problem in calculation of radiation field.

Recently, a novel and high-precision method for calculating the γ-ray build-up factor for multilayer shields has been proposed in this paper. The method is based on the deep neural network (DNN) [19, 20], which is a kind of machine learning. In this paper, the main works are to obtain the appropriate parameters that are related to the build-up factor calculation and construct an approximate deep neural network which calculates the build-up factor for multilayer shields by learning the relationship between parameters and the value of build-up factor. The methods not only can calculate a large number of build-up factors at one time but also its calculation accuracy is relatively high, which can meet the accuracy requirements of point-kernel code in the 3-D radiation field calculation and be applied into the practical engineering application.

In Section 2, it is a general description about the definition of build-up factor and introduction of some common calculation methods for MLBUF, and the novel and high-precision method is completely introduced in this section. Results and discussion are given in Section 3, and the method is validated by the MCNP, and a preliminary application is also illustrated. At the last, there is a conclusion about this work in Section 4.

2. Materials and Methods

2.1. Build-Up Factor. It is well known that build-up factor is a physical quantity describing the effect of scattered photons which makes the amount of received photons increase. Generally speaking, it refers to the ratio of the actual value of radiation quantities to the radiation quantities caused by the γ-ray, which is generated by the radiation source and does not react with the shields at the point of interest in the absorbed material. Build-up factors may refer to a number of various quantities. The physical quantities commonly used in radiation protection include flux, fluence, exposure, and dose, and the counterparts of build-up factors are flux build-up factor, fluence build-up factor, exposure build-up factor, and dose build-up factor. In the 3-D radiation field, the dose received by the staff is the key physical quantity to measure the radiation injury. Therefore, the work in this paper mainly considers the dose build-up factor among these build-up factors. The dose build-up factor is the ratio of the actual dose $\dot{D}$ at the point of interest to the dose D_1 produced by the γ-ray that does not interact with the material [21].

$$B = \frac{\dot{D}}{D_1}. \quad (5)$$

The methods for calculating the build-up factor for single-layer shields are well known. The methods mainly include analytical expression such as Taylor formula, Berger formula, and G-P fitting, tabulated form such as ANSI/ans-6.4.3 database. Compared with single-layer shields, the calculation of MLBUF is much more complicated, which not only depends on the characteristics of the current layer but also on the characteristics of previously penetrated layers. The early research studies on the calculation of MLBUF mainly focus on empirical formulas, and the empirical

formula established by Broder and his collaborators is commonly used, as shown in formula (2) [13]. Lin and Jiang proposed an empirical formula for the calculation of MLBUF, which is also one of the widely used empirical formulas as shown in formula (3) [15].

$$B\left(\sum_{i}^{N}\mu_i d_i\right) = B_N\left(\sum_{i}^{N}\mu_i d_i\right) + \sum_{i}^{N}\left[B_n\left(\sum_{i}^{N}\mu_i d_i\right) - B_{n+1}\left(\sum_{i}^{N}\mu_i d_i\right)\right], \tag{6}$$

where N is the number of shielding layers, B is the build-up factor of N-layer heterogeneous shielding media, and B_n is the build-up factor of homogeneous medium composed of nth shielding material.

$$B\left(\sum_{i=1}^{n-1}X_i, X_n\right) = B_n(X_n) + \left[B\sum_{i=1}^{n-1}X_i - B_n(X_n)\right] \times \left[K\sum_{i=1}^{n-1}X_i - C(X_n)\right], \tag{7}$$

where B_n is the build-up factor of nth shielding, X_n is the thickness of nth shielding, and K is shown in formula (8). If the high Z material is in front of the low Z material, the calculation of C is shown in formula (9), otherwise shown in formula (10) as follows:

$$K\left(\sum_{i=1}^{n-1}X_i\right) = \frac{B\left(\sum_{i=1}^{n-2}X_i, X_{n-1}\right)\left(\sum_{i=1}^{n-2}\right) - 1}{B_n\left(\sum_{i=1}^{n-1}X_i\right)1}, \tag{8}$$

$$C(X_n) = e^{-1.08\beta X_n} + 1.13\beta l(X_n), \tag{9}$$

$$C(X_n) = 0.8l(X_n) + \frac{e^{X_n}\gamma}{K}. \tag{10}$$

Although these empirical formulas can obtain good results at some extent in calculating the build-up factor for double-layer to quadruple-layer shields, the calculation by these empirical formulas needs some complicated parameters, which increases the complexity of calculation, and the range of application is limited and cannot meet the actual engineering application.

Suteau and Chiron introduced an iterative algorithm to calculate the build-up factor for multilayer shields in 2005 [17]. The algorithm is based on the empirical formula of double-layer shield build-up factor. In each iteration process, a single equivalent layer is used to replace the first two layers of shield materials, thus converting n-layer shields into $(n-1)$ layer shields. A large number of samples are trained to determine the atomic number and thickness of a single equivalent shield layer. Through a number of iterations, n-layer shields are transformed into double-layer shields, and the build-up factor is calculated by empirical formula of double-layer shield build-up factor.

The support vector regression method was proposed by Trontl et al. [18], which also transforms n-layer shields into $(n-1)$ layer through the iterative algorithm. Different from Suteau and Chiron's iterative method, the equivalent shield layer in each iteration process is calculated by support vector regression. The input vector space of SVR for single-layer and double-layer shields is obtained by the Monte Carlo method and SAS3 (Shield Analysis Sequence No.3), and the input vectors of SVR are the equivalent build-up factor of N layer (1,2, ..., N) in front of the shield layer and the build-up factor of the shield in the nth layer, the homogenized effective atomic number of (1, 2, ..., $N-1$) and the atomic number of the nth shield material, the equivalent shield thickness of the n-layer (1, 2, ..., $N-1$) in front of the nth shield layer and the shield thickness of the nth layer, and the incident photon energy. Finally, the build-up factor for multilayer shields is calculated by LIBSVM. According to Trontl's work, the relative average deviation (RAD) for the build-up factor of double-layer shields calculated by the support vector method is 9.7%, and the maximum relative absolute deviation is 68.77%, and RADs for triple-layer and quadruple-layer shields were 24.3% and 29.7%, respectively [18, 22].

Through the introduction of several common calculation methods of build-up factor for multilayer shields, it is found that although these methods can obtain good results and solve the problem of build-up factor calculation to a certain extent, the input vector space of the iterative method and support vector machine are incident photon energy, atomic number of shield material, shield thickness, and build-up factor for each shield, and the accuracy of the build-up factor calculated in this way cannot satisfy the requirements of the correction point-kernel code. In this paper, some new parameters are proposed as input vectors by studying the photon transport in the shields. The new parameters can effectively improve the calculation accuracy of build-up factor by training these parameters based on DNN.

2.2. Deep Neural Network. The deep neural network (DNN) is a kind of machine learning, which can be understood as a neural network with many hidden layers, and it is also well known as deep feed-forward network or multilayer perceptron. The structure of the deep neural network is divided into input layer, hidden layers, and output layer. The layers are fully connected, and any neuron in i layer must be

connected with any neuron in $i+1$ layer. The method based on DNN includes the following steps: the extraction of characteristics and features, procession of the features, internal training of samples, cross-validation, external test of samples, and so on. The structure of DNN applied in the method is shown in Figure 1.

2.3. Input Vectors. The input vectors are given by a number of parameters defining the physical problem that is to be modelled using the DNN.

2.3.1. Cross Section. To make the DNN learn characteristics of parameters of build-up factor more richly, the transport process of photons in the shield is analyzed in this paper. When γ-ray incidents on a shield, depending on shielding material (characterized by density and section of photoelectric effect, Compton scattering, and electron-positron effect) and photon energy, there exists a certain probability that the electromagnetic fields of photons interact with the electromagnetic fields of atoms, atomic electrons, nuclei, and charged particles. In the process of interaction, photons may be absorbed, and the whole energy of photons will be converted into other forms of energy. The scattering may occur and part of the photon energy will be absorbed, and its propagation direction will be changed, or the photon energy will remain unchanged, and only its propagation direction will be changed [23]. Any of the interaction process may result in secondary photons that have a probability of reaching the point of interest, thus increasing the flux, influence, or dose. In the process of interaction, the dominant interactions are photoelectric effect, Compton scattering, and electron-positron effect.

The photoelectric effect is the interaction of photons with bound electrons in matter, and the full energy of the photon is absorbed by a bound electron so that the kinetic energy of the electron is enough to get rid of the bondage of the atomic nucleus and emit from the inside of the atom, while the photon itself disappears. When the energy of the incident photon is high (above 1.022 MeV) and it passes by the nucleus, the incident photon may be transformed into a positron and a negative electron under the action of the nuclear Coulomb field. The reaction is called electron-positron effect. The incident photon collides with the material atom, and part of the photon energy is transferred to the external electron of the atom. The electron obtains kinetic energy and gets rid of the atomic bondage and becomes a recoil electron. The newly generated scattering photon deviates from the original direction, and its energy decreases.

When the energy of incident photon is relatively low, photoelectric effect dominates and then Compton scattering. While the energy of the incident photon is relatively high, the electron pair effect dominates. All matters obey this law. The probability of the three interactions between photons and materials is related to their cross section: cross section of photoelectric effect, Compton scattering, and electron-positron effect. According to the analysis, it can be deduced the three kinds of cross sections of interaction will directly affect the probability that the photons interact with the materials and affect the value of build-up factor. Therefore, using three kinds of cross-sections as input vector parameters can well reflect the physical process of photon transport.

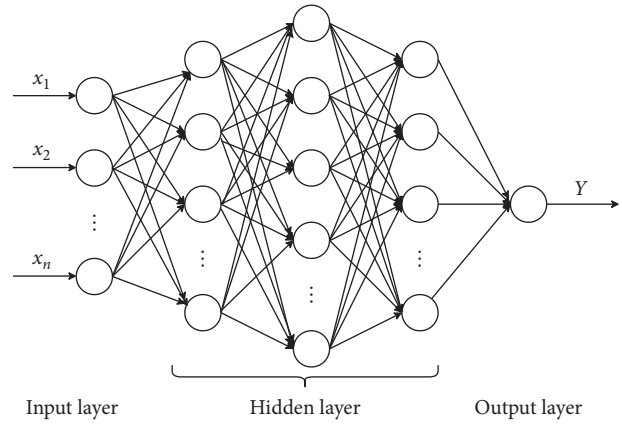

Figure 1: The structure of the deep neural network.

2.3.2. Energy of Incident Photons. The energy of incident photons also has a great influence on the calculation for build-up factor. When the energy of the incident photon is different, the corresponding three cross-sections for the same material are different and the build-up factor is also different. For the same shield, the build-up factor decreases with the increase in energy. The main reason is that the scattering cross section decreases with the increase in photon energy, which leads to the decrease in photon scattering.

2.3.3. Number of Mean Free Path. The number of mean free path (MFP) is an important parameter affecting the build-up factor, which is the ratio of photon penetration distance to mean free path. In shielding design, the thicker the shield is, the greater the number of the free path of photons in the shielding is, and the times of scattering are also more.

2.3.4. Density of Shield Material. The density of shield material is also one of the parameters affecting the calculation of build-up factor. The density of material is related to cross section in some way. For example, the quotient of density and cross section of shield material is the mass attenuation coefficient, which is the share of particles reduced by interaction after the charged particles penetrate through the unit mass thickness. The mass energy decreased coefficient and mass energy absorption coefficient are in the same way. In addition, the density can also be used as a representative of some material to distinguish the material through which photons penetrate for engineering application.

In conclusion, the input vector parameters of DNN include incident photon energy, material density of each layer, shield free path number of each layer, Compton scattering cross section of each layer, electron-positron effect cross section of each layer, and photoelectric effect cross

section of each layer. The input vectors and output of DNN are shown in Table 1.

2.4. MLBUF Calculation. According to the determined input vectors of DNN, the appropriate structure of DNN used to calculate the build-up factors is constructed. The DNN trains the sample data of build-up factor. By continuously adjusting the relevant parameters of DNN learning, the error of training set and verification set can meet the requirement of calculation accuracy of build-up factor. To ensure that the DNN learning does not appear overfitting and underfitting, the error of build-up factor of calculation training set and verification set is reduced as far as possible. The main flow chart of the build-up factor calculation method based on DNN is shown in Figure 2.

2.4.1. Learning Sample Data Generation. The Monte Carlo method has been used to generate the reference data points. According to the determined parameters to be learned, N groups of different shield models are established. Then, MCNP input files with different energy, different shield thickness, and different shield material combinations are generated in batch. The samples are calculated by MCNP program, and then the dose D considered the scattering photons calculated by MCNP, and D_1 unconsidered scattering photons are extracted in batches, and the corresponding build-up factors are calculated. After preprocessing the learning sample data, the learning sample data are divided into input items and corresponding output items.

2.4.2. Determine the Structure of DNN. The topological structure of the DNN is determined according to the number of input parameters and the number of output parameters. Considering the complexity of the practical shielding problem, the structure of DNN has the following guiding principles:

(a) For complicated engineering problems, the hidden layers of the neural network should adopt double-layer neurons as much as possible.

(b) In the single-layer hidden layer neural network, the structure of the neuron number of the whole neural network is recommended as follows:

$$n_1 \longrightarrow 2n_1 \pm 1 \longrightarrow n_2 \tag{11}$$

(c) In the double-layer hidden layer neural network, the structure of the neuron number of the whole neural network is recommended as follows:

$$n_1 \longrightarrow 1.5n_1 \longrightarrow 2n_1 \pm 1 \longrightarrow n_2. \tag{12}$$

According to the characteristics of build-up factor for multilayer shield calculation parameters, this paper adopts the following parameters of DNN to train the DNN:

(1) The deep neural network is composed of input layer, three hidden layers, and output layer

(2) The number of neurons in each layer is auto, 50, 80, 50, and auto

(3) Relu is selected as the activation function in the input layer and hidden layers, and linear is used as the activation function in the output layer

(4) SGD + momentum is adopted as the activation function as a training method, and the minibatch parameters are set to 512

(5) The ratio of training set, verification set, and test set is 9 : 1 : 1

2.4.3. Training and Prediction. The DNN is used to train the samples data. By adjusting the training parameters of the DNN, the relative average deviation of the training set and validation set is less than the setting accuracy or the iteration finished, and the DNN ends the training.

After the DNN finished the training, by inputting the input vectors (incident photon energy, material density of each layer, number of mean free path of each layer, Compton scattering cross section of each layer, electron-positron effect cross section of each layer, and photoelectric effect cross section of each layer), the build-up factor can be predicted quickly and accurately.

3. Results and Discussion

3.1. The Results. In this paper, the slab model and a point-collimated source are used as the calculation model of build-up factor, and the build-up factor for single-layer, double-layer, triple-layer, and quadruple-layer slab model is calculated, respectively. The geometry models of the four are shown in Figure 3, and the variation range of shield models is shown in Table 2.

By MCNP modelling, the problem of calculating the build-up factor is transformed into solving the ratio of the dose penetrated shields and the dose without considering the scattering. A number of MCNP input files are generated by random uniform sampling in the variation range of the shield layer. In this paper, the number of MCNP input files for single-layer, double-layer, triple-layer, and quadruple-layer slab model is 3900, 7800, 15600, and 31200, respectively. The build-up factor of each shield combination (each layer comprised of different material or a combination of materials) under different shields, different number of mean free path, and different incident photon energy is calculated.

The sample data are preprocessed for the DNN training. Then, the DNN trained the sample data, and the training iteration time of training is set to 100000. The DNN stops training until the validation set error converges to the ideal level. The mean absolute percentage error (MAPE) of training set and validation set is used as appraisal to the prediction, and the MAPE charts of the training process for single-layer, double-layer, triple-layer, and quadruple-layer slab model are shown in Figure 4. When the validation set error converges to the ideal level, the DNN stopped training, and the trained DNN was used to predict the build-up factor.

Table 1: Table of input vectors of DNN.

Layers	Input vector	Reference value
1	Energy, Density1, MFP1, Section of material 1	B1
2	Energy, Density1, MFP1, Section of material 1, Density2, MFP2, Section of material 2	B2
3	Energy, Density1, MFP1, Section of material 1, Density2, MFP2, Section of material 2, Density3, MFP3, Section of material 3	B3
4	Energy, Density1, MFP1, Section of material 1, Density2, MFP2, Section of material 2, Density3, MFP4, Section of material 3, Density4, MFP4, Section of material 4	B4
...	...	...

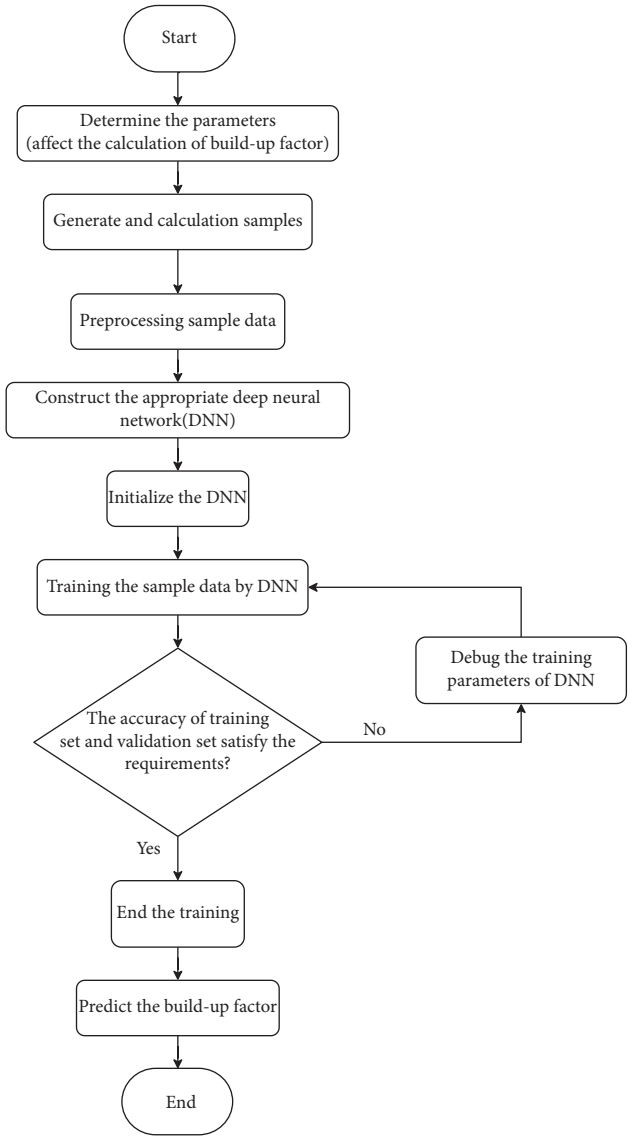

Figure 2: The flow chart of build-up factor calculation based on DNN.

$$\text{MAPE} = \frac{100\%}{n}\sum_{i=1}^{n}\left|\frac{\overset{\Lambda}{y_i} - y_i}{y_i}\right|. \tag{13}$$

3.2. The Regression Analysis and the Relative Average Deviation. The quality of the prediction was tested on all data (including training set, validation set, and test set), using relative average deviation (RAD) as a quality measure:

$$\text{RAD} = \frac{\left(\sum_{i=1}^{n}\left|y_i - f\right|/y_i\right) \times 100\%}{n}, \tag{14}$$

where f_i is the predicted value corresponding to the target value y_i.

The regression analysis on all data of training set, validation set, and test set has been done in this paper, and the results of single-layer shields, double-layer shields, triple-layer shields, and quadruple-layer shields are shown in Figure 5. According to the regression analysis chart, the DNN can well fit the parameters of the build-up factor, and there is no overfitting or underfitting. The relative deviation between the predicted value and the actual value calculated by MCNP is small and consistent.

For analysing the relative error between the predicted value and the target value, this paper has drawn the distribution of relative error of single-layer shields, double-layer shields, triple-layer shields, and quadruple-layer shields. As it is shown in Figure 6, the relative errors between all predicted values and actual values are mostly between −10% and 10%. It can be educed that the deep neural network is suitable for calculating the build-up factor. The RAD of different media of shielding is calculated, and the partial RAD results are shown in Table 3.

According to the results of comparison between predicted value and actual value, the relative average deviation observed for single-layer shields is 2.05%, with the maximum of 19.31% detected for a 0.141 mfp thick aluminum shield at 10 MeV incident γ-ray energy($B_{\text{MCNP}} = 1.049$ and $B_{\text{DNN}} = 0.846$). Only 0.57% of the predicted data points have the relative absolute deviation higher than 10%.

The RAD observed for double-layer shields is 2.87%. Maximum relative absolute deviation of 31.37% was observed for a shield composed of 0.199 mfp of iron and 0.026 mfp of aluminum, at 0.8 MeV γ-ray energy ($B_{\text{MCNP}} = 1.115$and$B_{\text{DNN}} = 1.464$). 2.05% of the predicted data points have the relative absolute deviation higher than 10%.

The RAD observed for triple-layer shields is 3.13%. Maximum relative absolute deviation of 32.50% was detected for a shield made of 0.078 mfp thick layer of iron with 0.712 mfp thick layer of aluminum followed by 0.061 mfp thick layer of iron at 0.6 MeV incident γ-ray energy ($B_{\text{MCNP}} = 1.460$ and $B_{\text{DNN}} = 1.934$). Only 3.25% of predicted

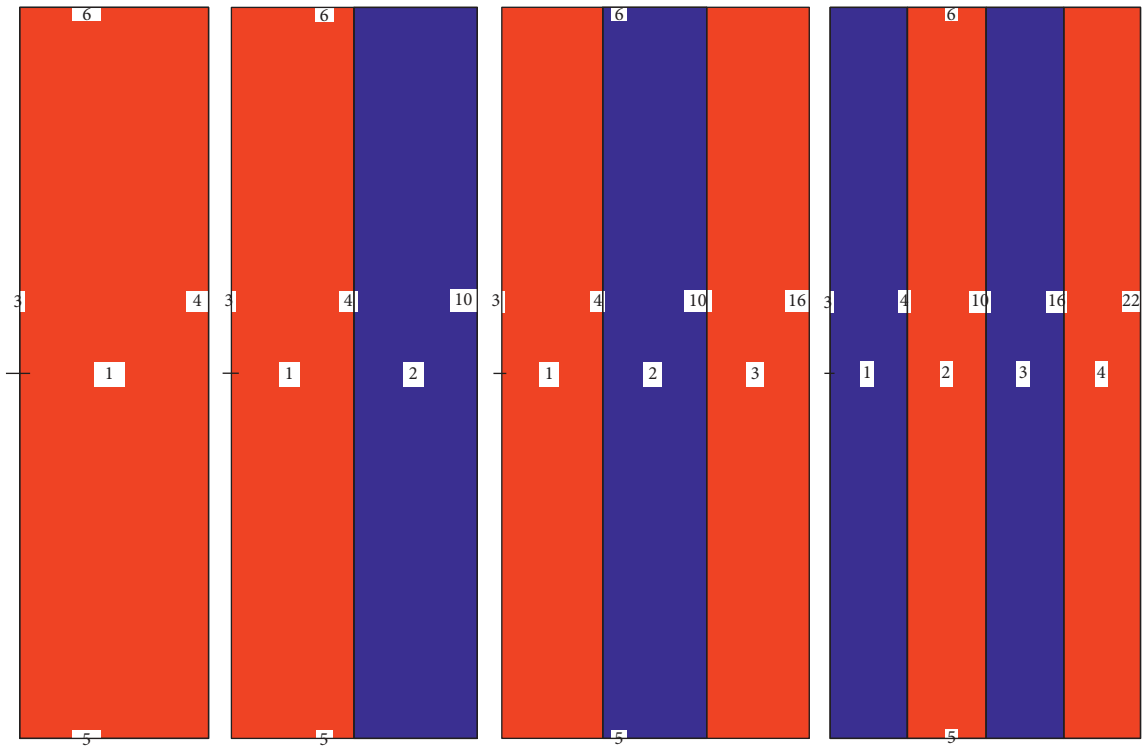

Figure 3: The schematic diagram of slab models.

Table 2: The variation range of the shield layer.

Shield layer	Total MFP of shield layer	Energy of incident photons (MeV)
Al	[0, 10]	{0.5, 0.6, 0.8, 1, 1.5, 2, 3, 4, 5, 6, 8, 10}
Pb + Fe	[0, 10]	{0.5, 0.6, 0.8, 1, 1.5, 2, 3, 4, 5, 6, 8, 10}
Fe + Al + Pb	[0, 10]	{0.5, 0.6, 0.8, 1, 1.5, 2, 3, 4, 5, 6, 8, 10}
Al + Fe + Pb + Fe	[0, 10]	{0.5, 0.6, 0.8, 1, 1.5, 2, 3, 4, 5, 6, 8, 10}

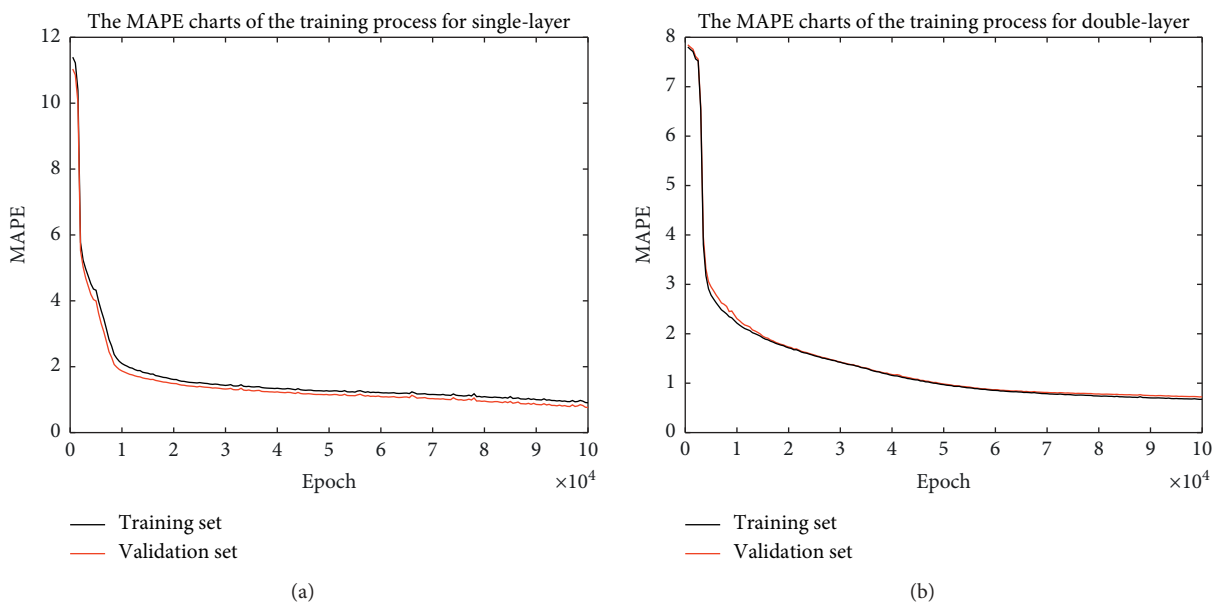

Figure 4: Continued.

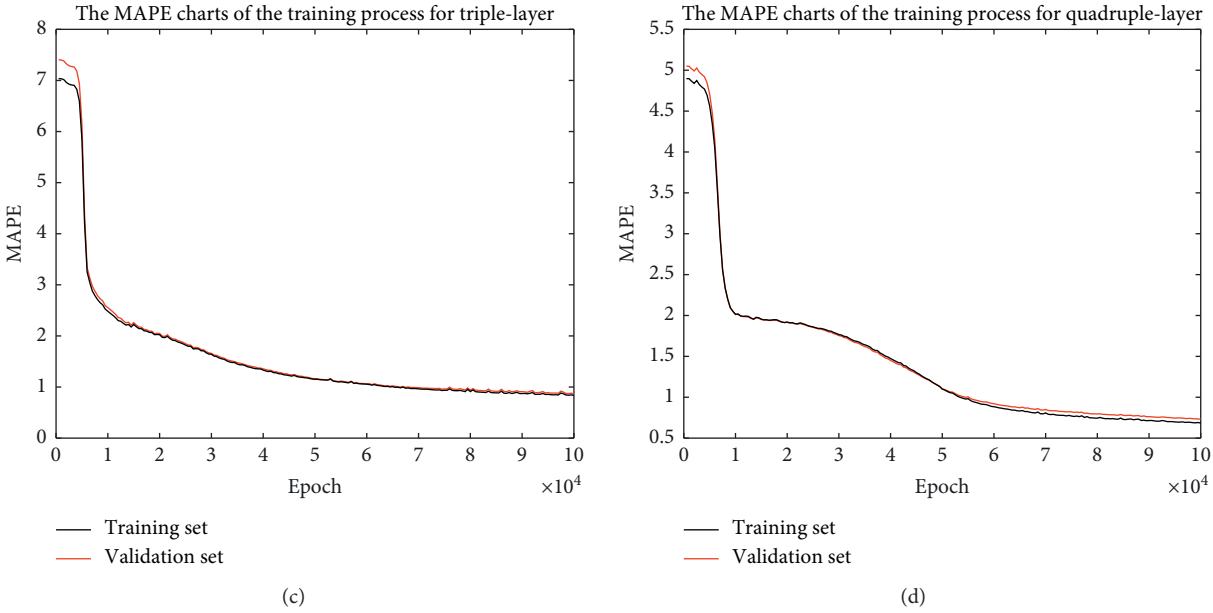

Figure 4: The MAPE of training set and validation set in the training process.

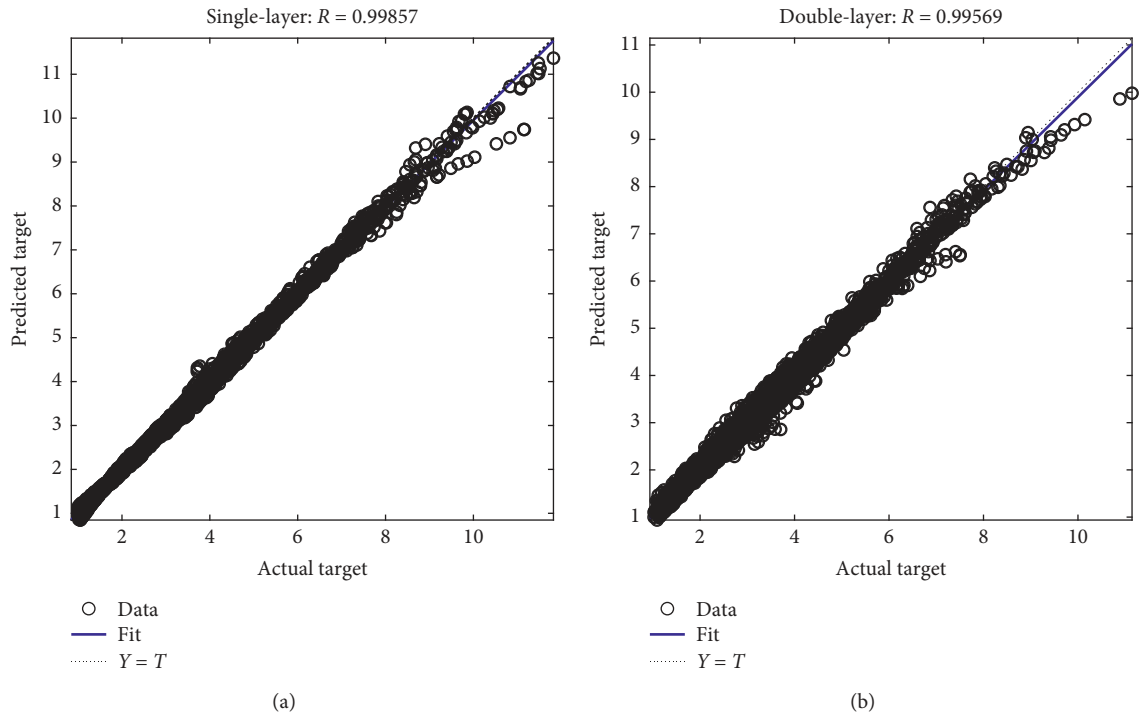

Figure 5: Continued.

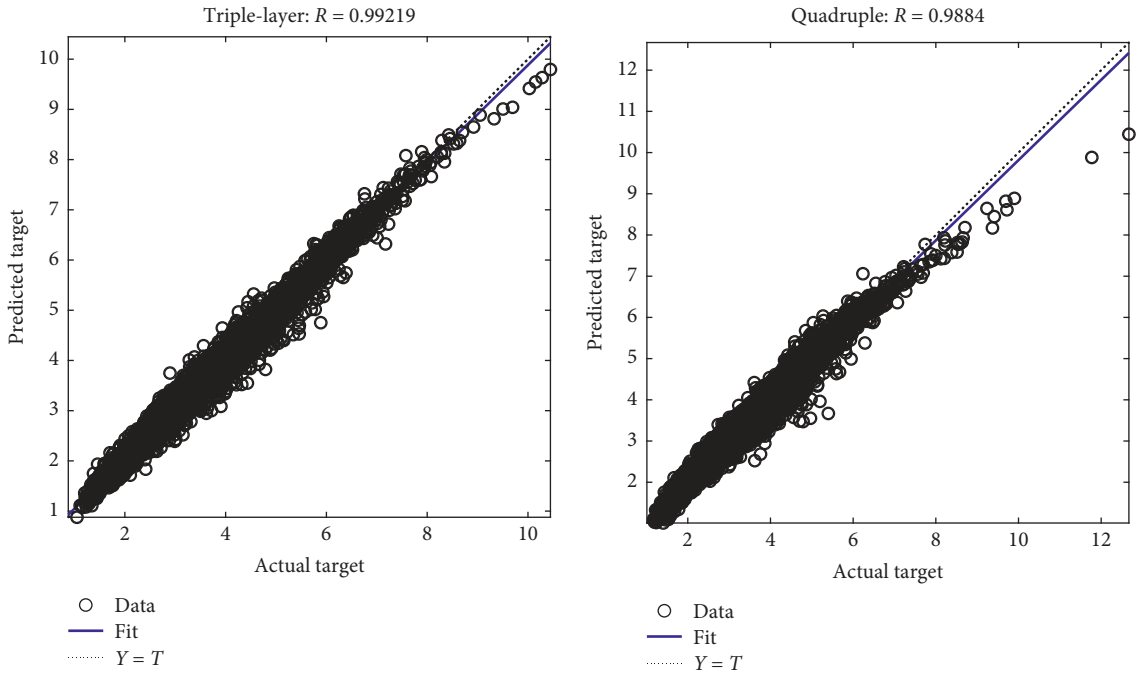

(c) (d)

Figure 5: The regression curve of all data.

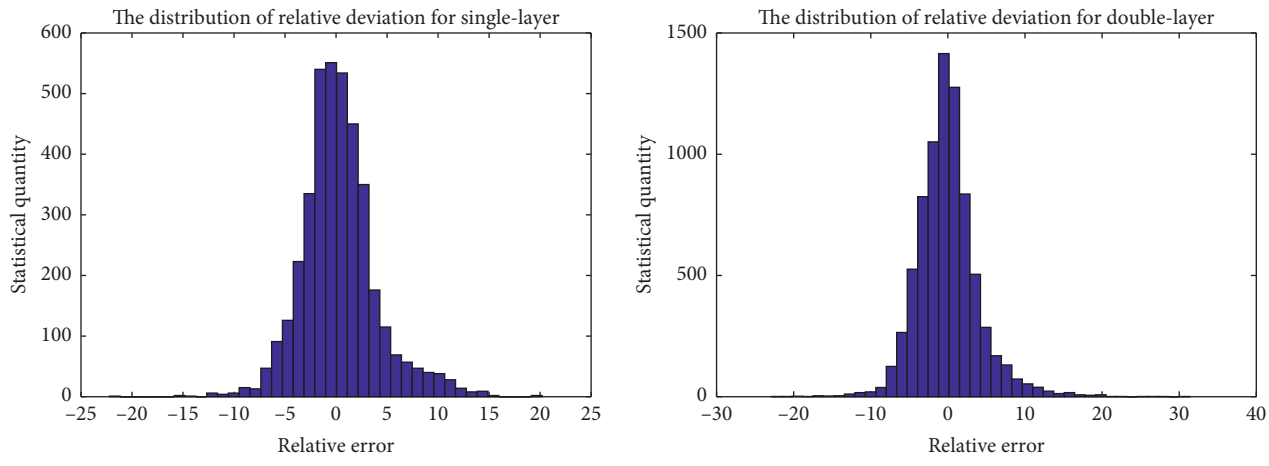

(a) (b)

Figure 6: Continued.

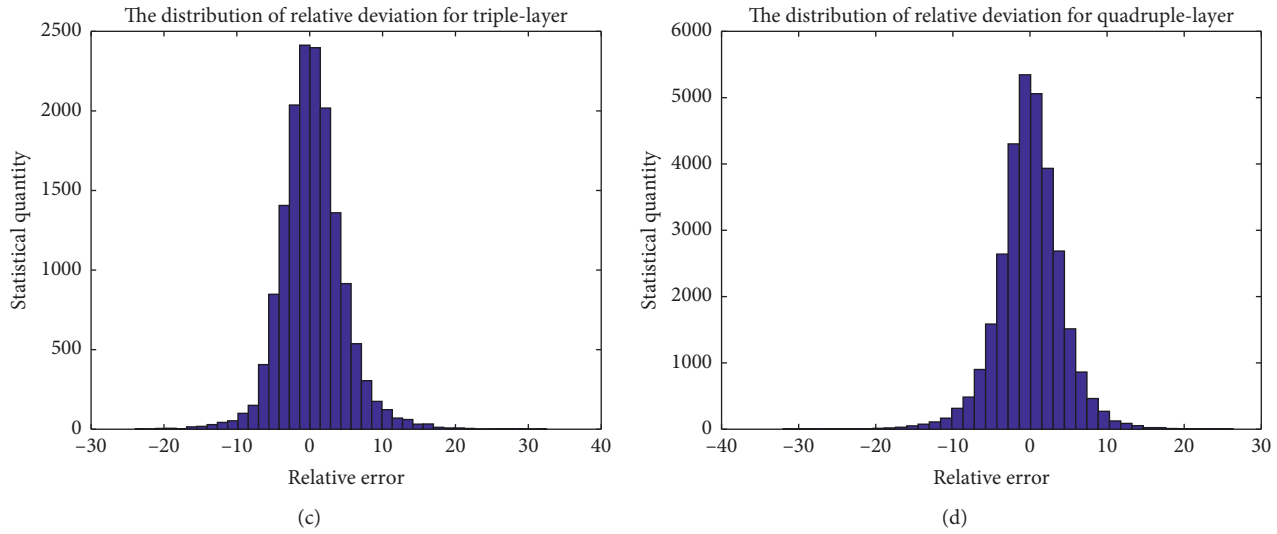

Figure 6: The relative error distribution.

Table 3: The partial RAD results.

Material of shields	Average deviation (%)	Maximum deviation (%)	Maximum deviation point ((MeV),[mfp1]...[mfpn])	Deviation >10 (%)
Al	2.20	19.31	(10, 0.141)	2.31
Fe	2.24	15.22	(10, 0.043)	0.69
Pb	1.71	12.71	(10, 9.870)	0.31
Al + Pb	2.65	20.21	(0.5, 4.489, 0.119)	1.27
Fe + Pb	2.48	22.18	(10, 0.022, 0.214)	1.64
Pb + Al	3.51	22.92	(10, 4.974, 0.281)	4.08
Al + Fe + Pb	3.05	20.24	(0.5, 3.218, 3.478, 0.186)	3.63
Fe + Pb + Al	2.83	19.32	(10, 1.755, 3.492, 0.214)	1.69
Pb + Al + Fe	2.90	21.30	(1, 2.195, 0.0796, 0.0538)	2.77
Al + Fe + Pb + Fe	2.69	17.50	(0.5, 2.233, 1.332, 0.143, 0.394)	1.54
Fe + Pb + Fe + Al	3.19	24.44	(0.6, 1.411, 2.468, 0.253, 0.078)	3.54
Pb + Al + Fe + Al	3.27	17.87	(0.5, 2.079, 0.419, 0.198, 2.074)	2.92

data points have the relative absolute deviation higher than 10%.

The RAD for quadruple-layer shields is 3.06%. Maximum relative absolute deviation of 32.04% was detected for a shield comprised of 2.259 mfp of aluminum, 1.689 mfp of iron, 2.137 mfp of aluminum, and 0.034 mfp of lead at 0.5 MeV γ-ray energy ($B_{\mathrm{MCNP}} = 5.399$ and $B_{\mathrm{DNN}} = 3.669$). Only 2.85% of predicted data point have the relative absolute deviation higher than 10%.

For validating the method, we re-establish an infinite homogeneous medium of the double-layer shielding model with a point-isotropic source and use the constructed DNN to train the MCNP sample data. This paper takes the MCNP value as reference value and compares the calculated results of DNN and Py-MLBUF with MCNP results at 3 MeV, respectively. The results of DNN at 3 MeV are calculated by the trained DNN, and the results of Py-MLBUF are calculated by the Py-MLBUF online platform. The calculation results of MCNP, DNN, and Py-MLBUF and the deviation of DNN results and Py-MLBUF results compared with the MCNP results are all shown in Table 4. According to Table 4, the RAD is 4.83% and the maximum relative absolute deviation is 18.39% for DNN and the RAD is 6.97% and maximum relative absolute deviation is 18.60% for Py-MLBUF.

3.3. The Comparison of Actual Target and Predicted Target. In this paper, the data (including training set, validation set, and test set) are been predicted by the trained DNN, and the partial predicted results of build-up factor for single-layer shields and stratified shields are showed in Figures 7 and 8. It can be seen that the curves of the predicted target and the actual target are almost identical, and the relative deviation is very small. The DNN constructed in this paper can fit the parameters of the build-up factor very well and calculate the corresponding build-up factor value successfully.

3.4. Application. The method has been preliminarily used in our 3-D radiation field calculation software called VMERAS

Table 4: The results of MCNP, DNN, and Py-MLBUF, and the deviation at 3 MeV.

Media of shield	MCNP	DNN	DNN Deviation: $\frac{\lvert DNN-MCNP\rvert}{MCNP}$	Py-MLBUF L&J	Py-MLBUF Deviation: (%) $\frac{\lvert L\&J-MCNP\rvert}{MCNP}$
2Al + 1Fe	3.09	2.87	7.12	2.98	3.56
2Al + 2Fe	3.82	3.65	4.45	3.66	4.19
2Al + 3Fe	4.60	4.48	2.61	4.41	4.13
2Al + 4Fe	5.29	5.27	0.38	5.21	1.51
2Al + 5Fe	6.14	6.03	1.79	6.05	1.47
2Al + 6Fe	7.06	6.72	4.82	6.94	1.70
2Al + 1Pb	2.63	2.25	14.45	3.06	16.35
2Al + 2Pb	3.14	2.93	6.69	3.67	16.88
2Al + 3Pb	3.71	3.63	2.16	4.40	18.60
2Al + 4Pb	4.51	4.36	3.33	5.20	15.30
2Al + 5Pb	5.22	4.86	6.90	6.04	15.71
2Al + 6Pb	5.98	5.56	7.02	6.93	15.89
2Fe + 1Al	3.18	2.90	8.81	3.22	1.26
2Fe + 2Al	4.03	3.89	3.47	4.06	0.74
2Fe + 3Al	4.85	4.59	5.36	4.89	0.82
2Fe + 4Al	5.68	5.19	8.63	5.73	0.88
2Fe + 5Al	6.57	6.06	7.76	6.58	0.15
2Fe + 6Al	7.41	7.50	1.21	7.44	0.40
2Fe + 1Pb	2.61	2.13	18.39	3.02	15.71
2Fe + 2Pb	3.14	2.77	11.78	3.65	16.24
2Fe + 3Pb	3.73	3.50	6.17	4.39	17.69
2Fe + 4Pb	4.57	4.29	6.13	5.19	13.57
2Fe + 5Pb	5.32	5.09	4.32	6.03	13.35
2Fe + 6Pb	6.12	5.99	2.12	6.92	13.07
2Pb + 1Al	2.91	2.93	0.69	3.14	7.90
2Pb + 2Al	3.80	3.87	1.84	3.90	2.63
2Pb + 3Al	4.69	4.80	2.35	4.68	0.21
2Pb + 4Al	5.55	5.34	3.78	5.48	1.26
2Pb + 5Al	6.43	6.22	3.27	6.31	1.87
2Pb + 6Al	7.34	7.44	1.36	7.16	2.45
2Pb + 1Fe	2.81	2.58	8.19	3.12	11.03
2Pb + 2Fe	3.61	3.54	1.94	3.87	7.20
2Pb + 3Fe	4.47	4.49	0.45	4.65	4.03
2Pb + 4Fe	5.36	5.36	0.00	5.46	1.87
2Pb + 5Fe	6.32	6.24	1.27	6.31	0.16
2Pb + 6Fe	7.27	7.47	2.75	7.20	0.96

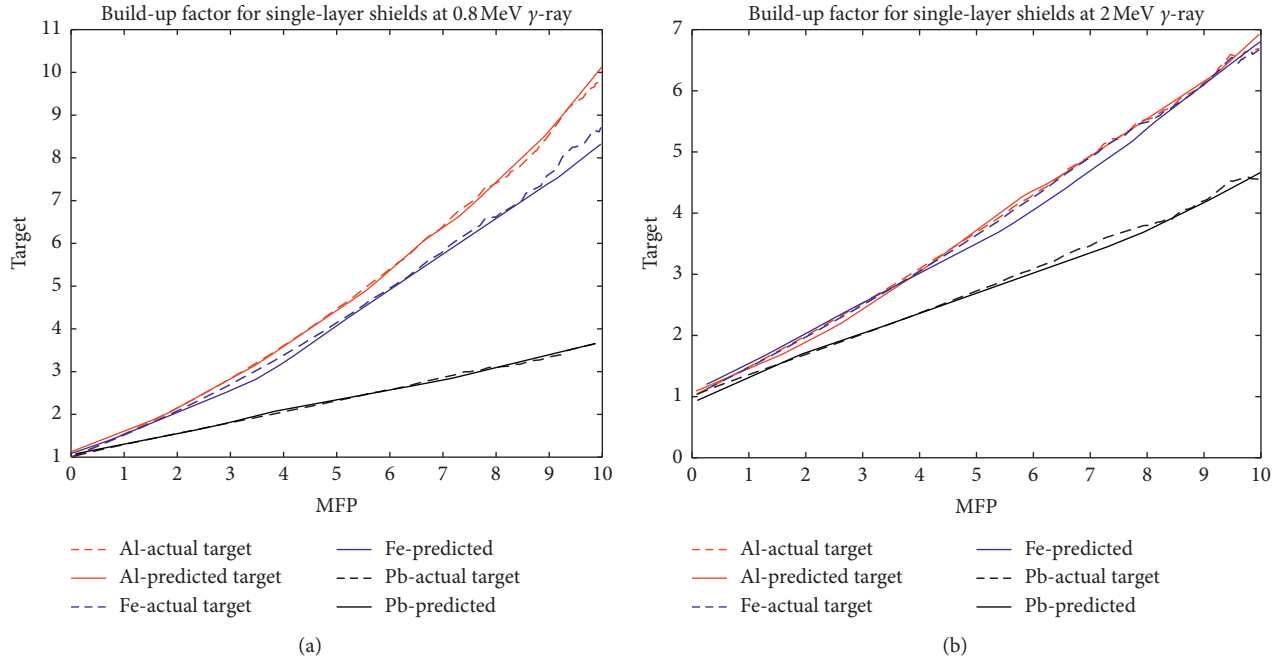

Figure 7: Continued.

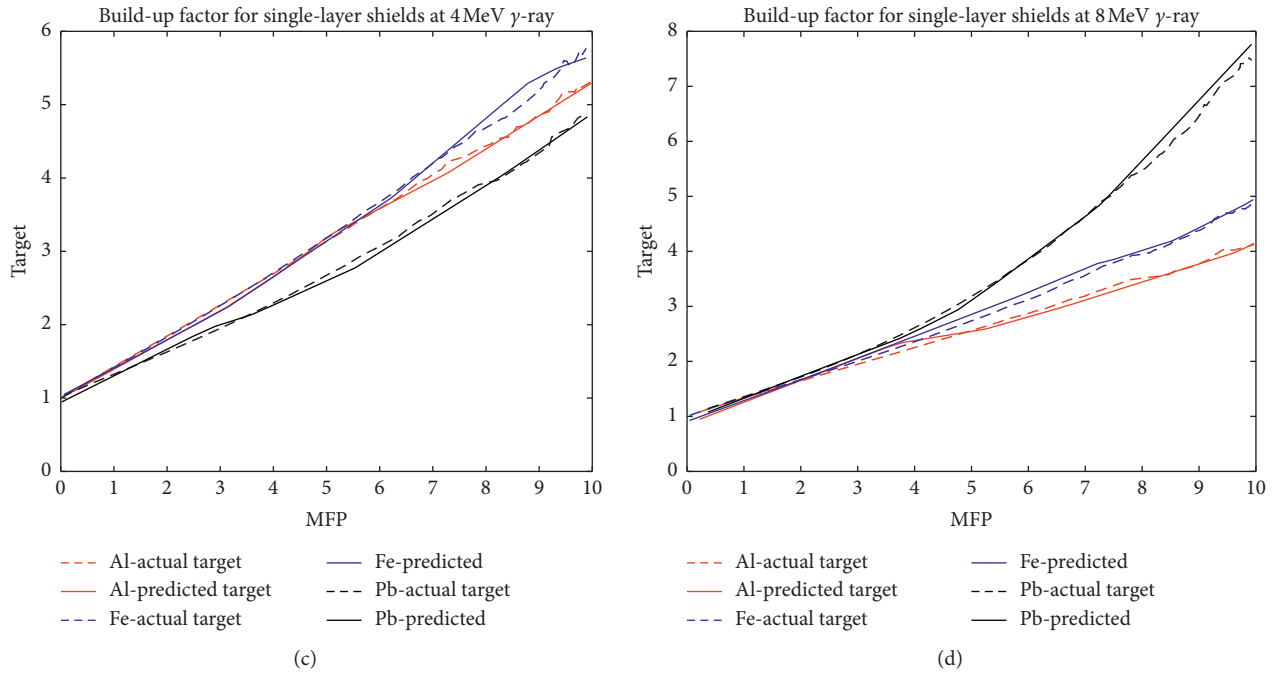

Figure 7: The comparison of build-up factor between actual target and predicted target for single-layer shields at 0.8, 2, 4, and 8 Mev γ-ray energy.

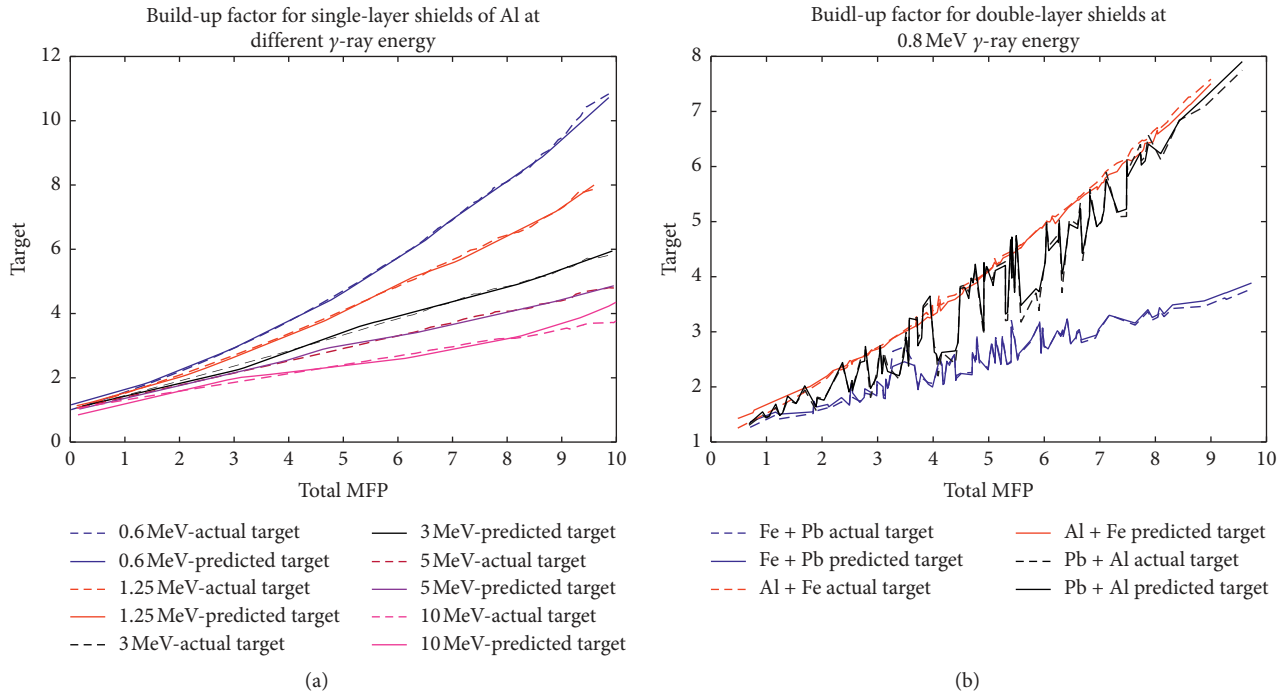

Figure 8: Continued.

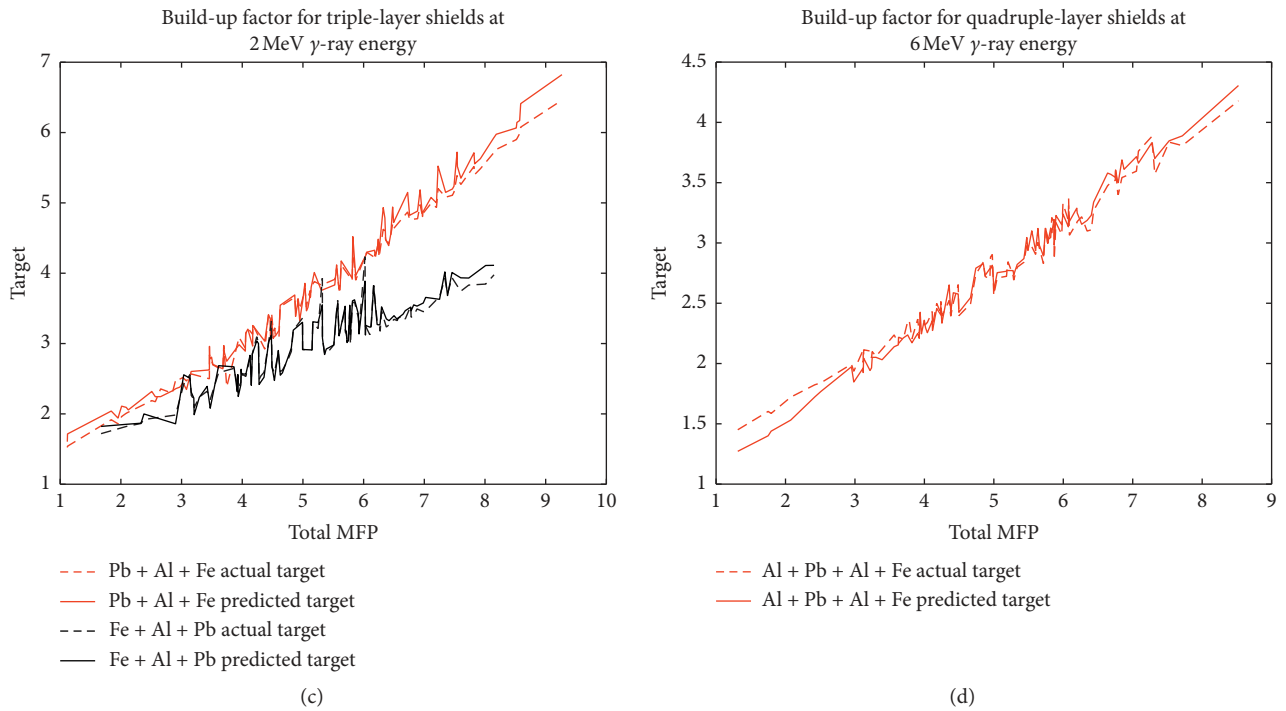

Figure 8: The comparison of build-up factor between actual target and predicted target: The comparison for (a) single-layer shields of aluminum at different incident photon energy, (b) double-layer shields at 0.8 MeV γ-ray energy, (c) triple-layer shields at 2 MeV γ-ray energy, and (d) quadruple-layer shields at 6 MeV γ-ray energy.

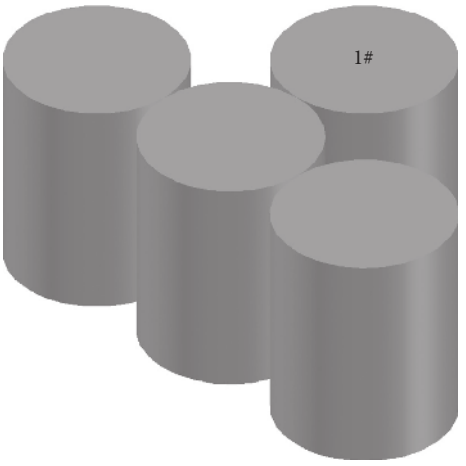

Figure 9: The CAD model display of the calculation model.

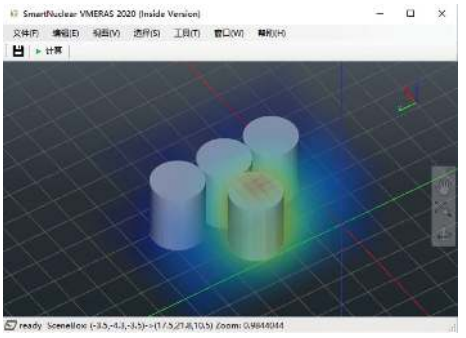

Figure 10: The visualization of the calculated radiation field.

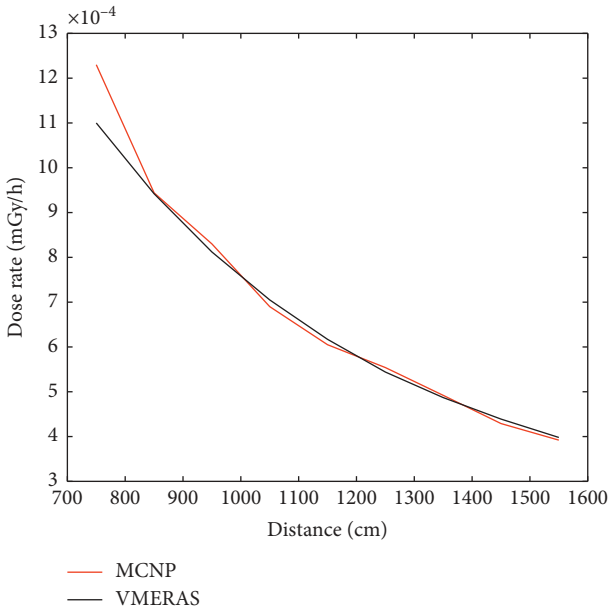

Figure 11: The comparison of calculated dose rate between MCNP and VMERAS.

as a sub module. This paper uses 4 simplified nuclear fuel waste barrels as the calculation model to calculate its 3-D radiation field, where #1 barrel is regarded as the source and the other barrels as shielding. Figure 9 is the CAD model display of the calculation model, and Figure 10 is the visualization of the calculated radiation field in VMERAS. Figure 11 is the comparison of partial calculated dose rate between MCNP and VMERAS. It can been clearly seen that the deviation between VMERAS and MCNP is very small, and it proved that the novel and high-precision method for calculating MLBUF has the ability to apply into the practical engineering.

4. Conclusion

In this paper, a novel and high-precision method for calculating the γ-ray build-up factor for multilayer shields is introduced. Comparing to the previous approaches, the biggest characteristics of the method are deep neural network and new parameters of the build-up factor calculation. Through the deep neural network constructed in this paper training the new parameters, the MLBUF can be calculated without decoupling the complex physical relationship between input and output. Once the deep neural network finishes the training, it can be used to predict a number of build-up factors in a short time. By illustrating the preliminary application case, it is proved that the novel and high-precision method has the ability to apply into the 3-D radiation field calculation program and it has a broad application prospect.

From the above discussion about the predicted results, it can be seen that the accuracy of the predicted build-up factor is very high and even the maximum deviation does not seem far from acceptable. The method can meet the accuracy requirement of point-kernel code correction in the calculation of 3-D radiation field and satisfy the requirement of calculation speed. Therefore, the method for calculating build-up factors is feasible in engineering practice.

Data Availability

The data used to support the conclusions of this paper are available from the corresponding author upon request.

Conflicts of Interest

The authors declare that they have no conflicts of interest.

Acknowledgments

This work was financially supported by the National Exemplary Base for International Science and Technology (grant no. 2018SYS04).

References

[1] I. M. Prokhorets, "Point-kernel method for radiation fields simulation problems of atomic science & technology," *Voprosy Atomnoj Nauki I Techniki = Pytannja Atomnoi Nauky I Techniky = Problems of Atomic Science and Technology*, vol. 48, no. 5, pp. 106–109, 2007.

[2] V. R. Cain and C. G. Qad, "A combinational geometry version of QAD-P5A,a point kernel code for neutron and gamma-ray shielding calculations," Report ORNI–CCC307, Radiation Shielding Information Center, Oak Ridge, TN, USA, 1977.

[3] Grove Software Inc, *MIROSHIELD® User's Manual*, Lynchburg, VA, USA, 2009.

[4] C. Dupont and J. C. Nimai, "MERCURE-4: a three-dimensional Monte Carlo program for the integration of straight-line attenuation point kernels," Report OLS SL-SN-82-116, International Atomic Energy Agency (IAEA), Vienna, Austria, 1980.

[5] Y. Guo, Y. Song, C. Lu, M. Fu, and Z. Zhang, "Monte calro-point kernel method for calculating the radiation field in decommissioning nuclear facilities," *Nuclear Science and Engineering*, vol. 38, no. 6, pp. 1002–1007, 2018, in Chinese.

[6] G. R. White, "The penetration and diffusion of Co60 Gamma-rays in water using spherical geometry," *Physical Review*, vol. 80, no. 2, pp. 154–156, 1950.

[7] Y. Harima, S.-i. Tanaka, Y. Sakamoto, and H. Hirayama, "Development of new gamma-ray buildup factor and application to shielding calculations," *Journal of Nuclear Science and Technology*, vol. 28, no. 1, pp. 74–84, 1991.

[8] J. J. Taylor, *Application of Gamma Ray Build-Up Data to Shield Design*, Westinghouse Electric Company, Pittsburgh, PA, USA, 1954.

[9] ANSI/ANS-6.4.3, *Gamma Ray Attenuation Coefficient and Buildup Factors for Engineering Materials, La Grange Park in Illinois*, American Nuclear Society, La Grange Park, IL, USA, 1991.

[10] Y. Harima, Y. Sakamoto, S. Tanaka, and M. Kawai, "Validity of the geometric-progression formula in approximating gamma-ray buildup factors," *Nuclear Science and Engineering*, vol. 94, no. 1, pp. 24–35, 1986.

[11] M. H. Kalos, "Nuclear Development Associates (NDA)," 1956.

[12] L. A. Bowman, D. K. Trubey, Bowman, and Trubey, "Oak ridge national laboratory, x–822," 1958.

[13] D. L. Broder, Y. P. Kayurin, and A. A. Kutuzov, "Transmission of gamma radiation through heterogeneous media," *The Soviet Journal of Atomic Energy*, vol. 12, no. 1, pp. 26–31, 1962.

[14] G. d. P. Burke and H. L. Beck, "Calculated and measured dose buildup factors for gamma rays penetrating multilayered slabs," *Nuclear Science and Engineering*, vol. 53, no. 1, pp. 109–112, 1974.

[15] U.-T. Lin and S.-H. Jiang, "A dedicated empirical formula for γ-ray buildup factors for a point isotropic source in stratified shields," *Radiation Physics and Chemistry*, vol. 48, no. 4, pp. 389–401, 1996.

[16] K. Mann and S. S. Mann, "Development of an online-platform for gamma-ray shielding calculations and investigations," *Annals of Nuclear Energy*, vol. 150, pp. 1–22, Article ID 107845, 2021.

[17] C. Suteau and M. Chiron, "An iterative method for calculating gamma-ray build-up factors in multi-layer shields," *Radiation Protection Dosimetry*, vol. 116, no. 1-4, pp. 489–492, 2005.

[18] K. Trontl, T. Šmuc, and D. Pevec, "Support vector regression model for the estimation of γ-ray buildup factors for multi-layer shields," *Annals of Nuclear Energy*, vol. 34, no. 12, pp. 939–952, 2007.

[19] G. E. Hinton and R. Salakhutdinov, "Reducing the dimensionality of data with neural network," *Science*, vol. 313, no. 5789, pp. 504–507, 2006.

[20] L. Ma, F. Juefei-Xu, F. Zhang et al., "Deep gauge: multi-granularity testing criteria for deep learning systems, automated software engineering," pp. 120–131, 2018, https://arxiv.org/abs/1803.07519.

[21] J. Fang, *Introduction of Radiation Protection*, China Atomic Energy Press, Beijing, China, 1991, in Chinese.

[22] P. Duckic, K. Trontl, and M. Matijevic, "Active Learning for Support Vector Regression in Radiation Shielding design," in *Proceedings of the International Conference on High Performance Computing & Simulation*, pp. 311–317, IEEE, Barcelona, Spain, July 2015.

[23] Z. Tian, *Radiation Dosimetry*, China Atomic Energy Press, Beijing, China, 1992, in Chinese.